Electronic structure of atomic adsorbates from x-ray-absorption spectroscopy: Threshold effects and higher excited states

E. O. F. Zdansky, A. Nilsson, H. Tillborg, O. Björneholm, and N. Mårtensson
Department of Physics, Uppsala University, Box 530, S-751 21 Uppsala, Sweden

J. N. Andersen and R. Nyholm
Department of Synchrotron Radiation Research, Institute of Physics, Lund University, Sölvegatan 14, S-223 62 Lund, Sweden
(Received 13 July 1992; revised manuscript received 11 December 1992)

Atomic C, N, and O chemisorbed on Ni(100) have been studied by x-ray-absorption spectroscopy. The atomic $2p$ orbitals are shown to form hybrid orbitals with the Ni $3d$ and $4sp$ bands. The spectral contributions from these hybrids are identified at the absorption threshold and in a region 6–12 eV above this. Between those regions, states derived from atomic $3p$ and higher np orbitals are observed. The threshold region shows vibrational and dynamical effects, which are discussed in connection with the corresponding photoemission spectra. The substrate Ni $2p_{3/2}$ x-ray-absorption spectrum is also presented. Its large similarity to the Ni $2p_{3/2}$ x-ray photoemission spectrum is discussed.

I. INTRODUCTION

Core-level spectroscopy provides a method to study the local electronic structure around an atomic site. This is particularly useful in studies of adsorbed atoms and molecules on surfaces, since the electronic states on the adsorbate are often difficult to separate from the substrate states. Using x-ray-absorption spectroscopy (XAS), also denoted near-edge x-ray-absorption fine structure (NEXAFS), the unoccupied states on the adsorbate are probed.[1,2] From core-hole decay processes such as observed in soft x-ray emission spectroscopy[3] and Auger and autoionization spectroscopy[4] the local occupied electronic states can be studied. Local valence excitations between these different states can be observed in the core-level photoemission shake-up satellites.[5]

XAS utilizing polarized synchrotron light has been widely used to extract the orientation of molecules on surfaces.[1] In the case of adsorbed atoms the local geometry has been derived by comparing x-ray-absorption (XA) spectra taken up to 50 eV above threshold with multiple-scattering calculations.[6] In order to fully use XAS as a method to obtain information regarding the electronic structure of adsorbates there are a number of effects which need to be understood in some detail. These are, for example, the position of the Fermi level in the spectra, core-hole-induced modification of the density of states, dynamical effects at threshold due to metallic screening, vibrational motion, multielectron satellites, existence of higher excited Rydberg-derived states, and the perturbation upon these due to the presence of the surface. Recently, these phenomena have been addressed in the case of molecular adsorbates on various metallic substrates.[2,7,8] The present paper deals with these effects for atomic adsorbates from low Z elements. Contrary to many molecular adsorbates the chemisorption bond strength is of the same order of magnitude as the cohesive energy of the substrate. This represents the case of extremely strong chemisorption. We have chosen to study atomic C, N, and O on Ni(100) since these adsorbates have been well characterized in the past and the change in the XA spectra with atomic number and thereby the $2p$ occupation can be nicely followed.

The C, N, and O overlayers on Ni(100) have been extensively studied concerning the structure and vibrational properties.[6,9–20] All three atomic adsorbates form ordered surface structures at a coverage of one-half of a monolayer. The adsorption of O leads to the formation of a $c(2\times2)$ structure in which the O atoms occupy fourfold hollow sites 0.9 Å above the surface. The adsorption of C and N leads to a reconstruction of the substrate, giving rise to a primitive (2×2) structure having $p4g$ space-group symmetry. The carbon and nitrogen atoms penetrate the top Ni layer into hollow sites, which are located only 0.1 Å above the surface nickel atoms. The space becomes available through an opening of the first Ni layer by alternating clockwise and counterclockwise rotation of the four Ni atoms surrounding the adsorbate atoms.

The electronic structure of these strongly adsorbed species has only to a limited extent been studied, and the studies have mainly been concentrated on O adsorption. A comparative study of the three adsorbates has recently been performed by angular-resolved photoemission.[21] The adsorbates show occupied $2p$-derived levels with band dispersions located from 5 to 7 eV below the Fermi level. The adsorption of C and N show some additional states in the region of the Ni d band close to the Fermi level. The unoccupied states have only been studied for O using inverse photoemission, revealing the presence of an O-derived feature close to the Fermi level.[22] A comparative core-level shake-up study of C, N, and O revealed significant differences between the different adsorbates.[23] It was shown that the satellites are due to local excitations on the adsorbate, and not to excitations within the substrate. The major satellites were assigned

to $2p \rightarrow np$ excitations.

In this paper we will first present a general discussion of the various aspects of XAS known from studies in the bulk and for free atoms and molecules. Particular attention is paid to the dynamical response to the creation of the core hole, leading to a spectral singularity at threshold, and vibrational effects. New high-resolution XA spectra for C, N, and O on Ni(100) are presented. These are interpreted in terms of hybrid states formed between the atomic $2p$ and higher np Rydberg orbitals and the Ni $3d$ and $4s,p$ bands.

II. EXPERIMENT

The x-ray-absorption measurements were performed at the MAX-I synchrotron radiation facility in Lund, using a modified Zeiss SX-700 monochromator.[24,25] The absorption spectra were measured in the partial electron yield mode using a pulse-counting channeltron detector. The retarding grid was set to -200, -300, and -400 V for C $1s$, N $1s$, and O $1s$ decay electrons. In the detailed edge spectra, the photon-energy resolution was set to about 0.2 eV for C $1s$ and N $1s$ and 0.3 eV for O $1s$. For the more extended regions the resolution was set to 0.4, 0.3, and 0.5 eV for C $1s$, N $1s$, and O $1s$, respectively. The absolute value of the photon energy was determined using two different methods. First, the $2\pi^*$ resonance positions for condensed CO multilayers were measured. These positions are well known from electron-energy-loss measurements in the gas phase and amount to 287.40 and 534.20 eV for C $1s$ and O $1s$, respectively.[23,26] Second, we used the fact that the difference in kinetic energies of photoelectrons excited by first- and second-order light is exactly the photon energy of the first-order radiation. The accuracy of these photon-energy determinations are estimated to be about ± 0.1 eV. The spectra were normalized by dividing with spectra recorded for the clean surface. The x-ray photoemission spectroscopy (XPS) measurements were performed in Uppsala with an overall resolution of 0.3 eV and absolute binding energies within ± 0.1 eV.

The Ni crystal was cleaned by Ar^+ sputtering and annealing in vacuum or oxygen. The cleanness of the surface was monitored by Auger electron spectroscopy, XPS, and XAS. The temperature was measured by using a chromel-constantan thermocouple spot welded to the edge of the crystal. The adsorbate layers were formed by adsorption and thermal decomposition of C_2H_4, NH_3, and O_2. The ordering of the adsorbate layers were monitored by low-energy electron diffraction.

III. SPECTRAL SHAPES IN XAS

A. One-electron description

Before describing the x-ray-absorption process we will present a schematic picture of the $2p$ density of states for an atomic adsorbate, which could be carbon, nitrogen, or oxygen on Ni. Figure 1 shows an illustration of the one-electron $2p$ density of states with the occupied part to the left and the unoccupied part to the right separated by the Fermi level. Slab calculations using the local-density approximation and the linearized-augmented-plane-wave method have been performed for O on Ni(100).[27,28] The results show bonding states 5.5 eV below the Fermi level. These have a large O $2p$ character, which is mainly hybridized with Ni $4sp$ states. Antibonding states with O $2p$-Ni $3d$ character are found centered at the Fermi level. The occupied part of these states have been observed experimentally using photoemission[29] and x-ray emission,[3] while the presence of empty oxygen states at the Fermi level has been suggested from an inverse photoemission study.[22] The calculations show some indication of $2p$-derived states well above the Fermi level.[27] The presence of such states is supported by comparison with studies of various transition-metal oxides, which also indicate the existence of O $2p$ states extending up to 15 eV above the Fermi level.[30] These states have been attributed to antibonding O $2p$-metal sp hybrid orbitals. Calculations of the electronic structure of carbon on Ni(100) have been performed using slab models.[31,32] The gross features are similar to those of oxygen adsorption.

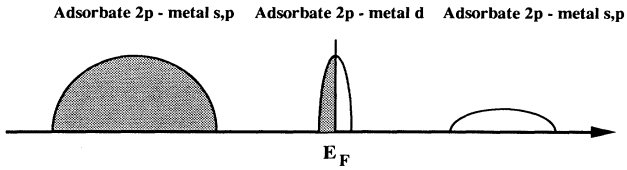

FIG. 1. Schematic one-electron $2p$-derived local density of states for an atomic (C, N, O) adsorbate on the surface of a transition metal, such as nickel.

From these considerations we can expect two different regimes of empty $2p$ states: a relatively narrow band at the Fermi level dominated by hybridization with Ni $3d$ states and a broad band due to antibonding combinations with Ni $4sp$ states high up in the continuum.

The XA spectral shapes are to a first approximation given by the unoccupied part of the density of states. Due to the local character of the transition only the projected density of states at the core excited site is probed. Furthermore, since the transitions are due to dipole excitations only certain substates of this projected density of states contribute to the spectra. This can be formulated in terms of more or less strict selection rules where it is important to consider the total symmetry of the initial and final state.[33] However, since the absorption matrix elements are much dominated by the character of the valence orbitals close to the nuclei where the core orbitals are located, the transitions can to a good approximation be described in terms of the atomic character of the valence orbitals, i.e., atomic dipole selection rules can be used. Hence the photoabsorption from the $1s$ shell should only project out those parts of the unoccupied band which have atomic p symmetry in an expansion at the excited site. Furthermore, since the important parts of the wave functions are little affected by the chemical environment atomic matrix elements can be used. This approximation has been tested in the case of x-ray emission and has been found to give a reasonably good description of the spectral intensities (within 70–80 %).[34] For higher states with the same symmetry the transition

matrix elements will be successively smaller as the principal quantum number increases. These contributions, however, should be present somewhere in the spectra. The $3p$ states especially could be visible since the much smaller matrix elements for the $3p$ final states compared to the $2p$ states are partly compensated by the fact that $3p$ is totally empty while the $2p$ orbital is largely occupied.

The transition matrix elements are also sensitive to the symmetry of the total adsorbate system, or less strictly on the local symmetry of the core-excited site. For $1s$ to valence-p excitations in atomic adsorbates only p_x and/or p_y components can be reached with normal incidence of the radiation. In grazing incidence with the polarization vector nearly perpendicular to the surface, excitation to a p_z level will instead be enhanced[35] (p_z is perpendicular to the surface).

When treating core-level processes in solids the final-state rule has been found to apply.[36,37] According to this rule the observed states in XAS are eigenstates of the system with the core hole present. The core hole may lead to significant modifications of the spectra relative to the initial-state electronic structure. In a static final-state picture the spectrum is related to the (symmetry-projected) partial density of empty states for the system with a core hole. In metallic systems various schemes have been used to treat the core-hole effects. A particularly convenient treatment in some cases is to replace the core excited atom by a $Z+1$ atom, i.e., the core hole is simulated by an extra nuclear charge. This approximation is, in general, sufficiently good, although in some cases there are coupling effects between the open core shell and the outer valence electrons which are not included in such a treatment and the atomic geometry may be slightly different. The $Z+1$ approximation can be applied using both experimental spectroscopic data for the $Z+1$ element and calculations.

B. Dynamical effects

The fact that the core hole modifies the electronic structure implies that a simple one-electron picture is not sufficient even if it is based on a system with the core hole present.[37–40] It is important to consider the dynamic response due to the creation of the core hole. Model calculations have been performed for the case of a homogeneous electron gas.[37] The calculations for these systems show that the dynamic response tends to build up a singularity at the Fermi level which is tailing off towards higher absorption energies. Based on these model calculations the final-state rule as formulated above has been extended to claim also that the singular response near threshold can be accurately described by multiplying the one-particle result with power-law factors, one for each angular-momentum channel contributing to the spectrum. There is also an important sum rule which states that the integrated intensity of the dynamical spectrum is equal to that of the static initial-state spectrum.

When XAS is used to investigate the empty valence states of a system it is essential to establish which photon energy corresponds to transitions to the Fermi level. For metallic systems the corresponding XPS core-level positions can be used.[2] The totally screened XPS final state is for all practical purposes identical to the lowest photoabsorption final state. The difference due to the fact that one electron is actually removed from the system in the XPS process but not in XAS is truly negligible because this will only change the Fermi level by an amount inversely proportional to the total number of valence electrons in the system. For metallic systems this effect can be totally neglected. In practice, the experimental XPS peak position can usually be used. However, the formally correct binding energy refers to that particular state in the XPS profile which corresponds to the totally screened situation. The core electron lines in metallic systems are always asymmetric due to shake-up processes. This has been treated theoretically with the same type of method as for the dynamical response in XAS and model line profiles have been derived. Using such profiles the measured spectra can be fitted and the appropriate XPS positions can be derived. The influence of vibrations on this procedure will be discussed in Sec. III C.

The essential influence of the dynamic effects is schematically described in Fig. 2. The nonshaded part of the figure shows the density of states in the presence of the core hole. This gives to a first approximation the spectral shape. However, more correctly the spectral shape is obtained by considering for each possible final state the dipole transition element between the initial-state wave function and that particular final-state wave function. Relative to the partial density of states this may modify the spectrum, for instance, as illustrated in Fig. 2 with the addition of the shaded region. The exact form of the shaded area will depend on the density of states. Provided that the sum rule, as discussed above, applies, the area of the shaded region will be proportional to the decrease in unoccupied density-of-states electron count on the creation of the core hole. In other words, the relative intensity of the shaded area will, in principle, tell how much the population of the probed orbital increases when a core hole is created. This relative intensity is $(n_i - n_f)/n_i$, where n_i and n_f are the number of empty states in the initial and final state, respectively, of

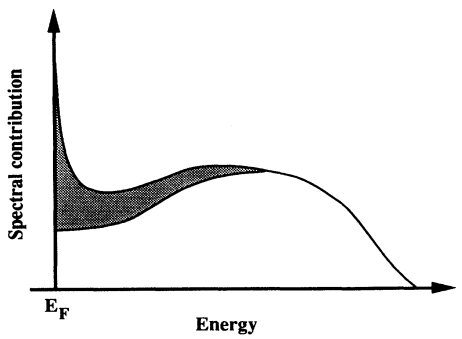

FIG. 2. Dynamic threshold effects in x-ray-absorption spectra. The nonshaded area represents the unoccupied density of states in the presence of a core hole. The observed spectrum is modified by dynamical effects represented by the shaded area.

the particular orbital probed. In the case of an essentially unfilled band (n_i large) the shaded fraction of the area in Fig. 2 will be relatively small. However, in a system which is close to having a filled band the situation is different. If the creation of the core hole leads to a filled band there are essentially no empty states ($n_f \approx 0$) in the final state and the shaded region may completely dominate the spectrum.

In order to demonstrate the effects discussed above it is instructive to consider a system with close to one hole in a valence shell. Ni metal is such a case with approximately a $3d^9$ valence electron configuration. The one-electron initial-state spectral shape for the $2p$-$3d$ photoabsorption process is given by the empty Ni $3d$ partial density of states. In the presence of a core hole the Ni $3d$ band will be essentially full ($3d^{10}$) as it is in Cu (the $Z+1$ element). In a static one-electron final-state picture the $2p$-$3d$ photoabsorption spectrum would then be practically nonexistent. If the $3d$ shell becomes totally closed in the final state there is only one $2p$-$3d$ transition possible, i.e., the transition is energetically well defined. All the $2p$-$3d$ spectral weight will then be contained in this transition, and a single peak will be seen in the photoabsorption spectrum. One may also express this in terms of a singularity which is dominating the spectrum completely. According to the intensity sum rule the intensity of this transition is given by the number of empty $3d$ states before the core excitation. In this case, it is evident that the Fermi level is not at all located halfway up on the leading edge. Since the photoabsorption final state more or less corresponds to one single state, this should be the Fermi level, i.e., the Fermi level is more associated with the peak position in the XA spectrum.

In Fig. 3 the $2p$ XP and XA spectra are compared for Ni. Both spectra have been accurately calibrated. In the XA spectrum the photon energy is given while the XP spectrum is plotted on a binding-energy scale relative to the Fermi level. It is immediately clear that the spectra

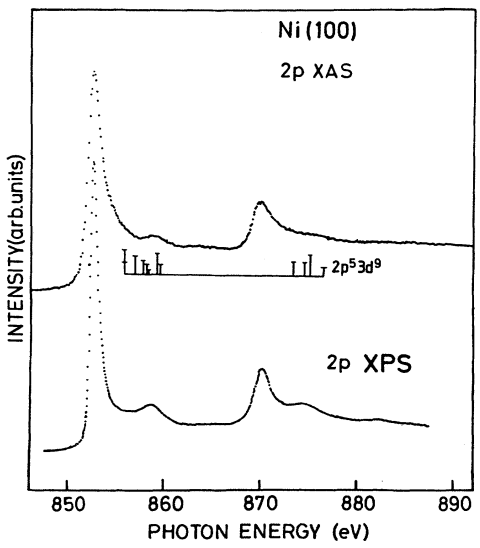

FIG. 3. Ni $2p$ XA and XP spectra. The multiplet pattern of the $2p^5 3d^9$ satellites is taken from Ref. 49.

are very similar. The peak positions coincide and the complete spectral shapes show the same characteristic signatures including the well-known 6-eV core-level satellite. The satellite intensities in the spectra are, however, different. This is the case since the full processes are different, i.e., in XPS the core electron is totally removed from the system while in the XA final state the electron is excited to the valence shell. Ni $2p$ XA spectra are influenced by adsorbates.[41,42]

C. Vibrational excitations

The perturbation caused by the core excitation also modifies the bonding of the excited atom to the lattice.[5] If the equilibrium bond distance changes, this leads to vibrational excitations which can be described by a Franck-Condon–type of treatment. The vibrational broadening will be similar for the XPS main line and the photoabsorption edge, since the electronic states are similar, as discussed above. The edge will thus be broadened by a function which corresponds to the XPS vibrational profile. The higher final states in the photoabsorption process will induce other changes in the potential-energy surfaces and thereby other vibrational line profiles.

IV. RESULTS AND DISCUSSION

A. Threshold region

In Figs. 4–6 the threshold regions are shown for the $1s$ photoabsorption spectra for C, N, and O adsorbed on

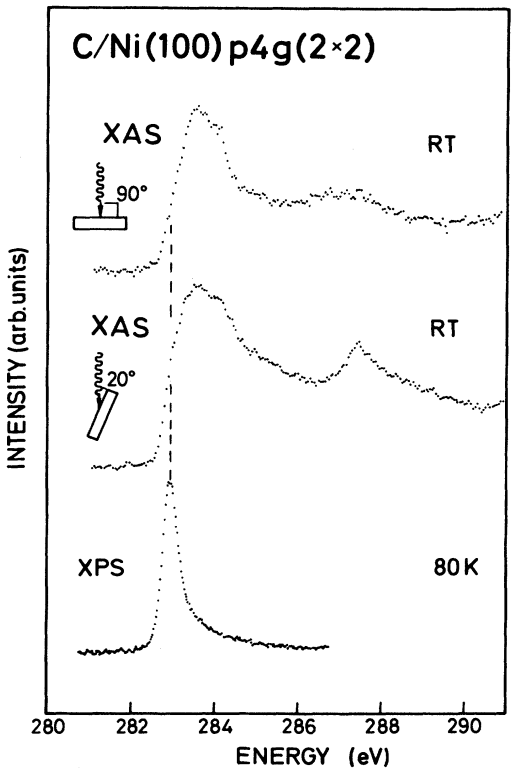

FIG. 4. XA and XP spectra for $p4g(2\times2)$ C/Ni(100). For the spectra in Figs. 4–6 the sample was cooled by liquid nitrogen (LN) unless otherwise indicated (RT=chamber temperature).

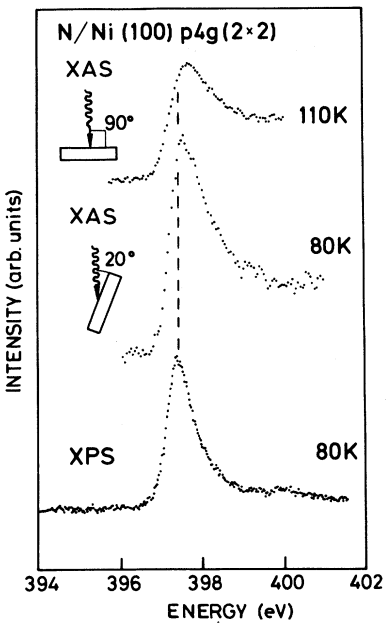

FIG. 5. XA and XP spectra for $p4g(2\times2)$ N/Ni(100). See also Fig. 4.

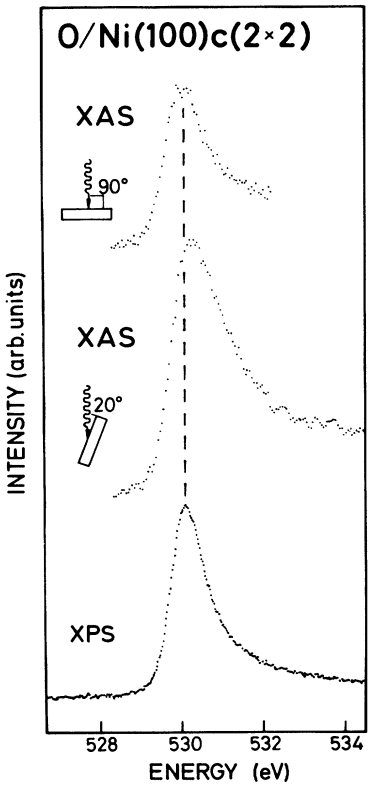

FIG. 6. XA and XP spectra for $c(2\times2)$ O/Ni(100). See also Fig. 4.

Ni(100), respectively. The spectra have been recorded both for light which is incident normal to the surface and at 20° grazing angle. The intensities for one pair of angles are normalized against the background below the edge. For molecular adsorbates this procedure was found to give the angular intensity dependence expected from dipole selection rules. The spectra are furthermore compared to the XP core-level spectra. The photon-energy scales for the XA spectra are aligned to the binding-energy scales relative to the Fermi level for the XP spectra. In all the XA spectra there are strong features at the Fermi level. The general appearance of the individual edge peaks are, however, rather different. The peaks have different line shapes and line positions relative to the core-level binding energies. The threshold peaks are generally stronger for grazing incidence and, in addition, they also show some other changes.

The edge peak for carbon is about 2 eV broad. The corresponding C 1*s* feature in XPS has a full width at half maximum (FWHM) of only 0.47 eV. The edge peak contains several characteristic features. In the rising edge a structure is clearly seen, which within the experimental accuracy coincides exactly with the XPS C 1*s* position. For grazing incidence this structure has higher intensity than at normal incidence. This difference makes the core-level binding-energy position in carbon fall halfway up on the edge at grazing incidence and nearly at the bottom of the edge for normal incidence. The relative intensities of the other components are also polarization dependent.

The edge peak for nitrogen is considerably narrower than for carbon. The N 1*s* peak in XPS, however, is broader (FWHM $=0.79$ eV) than the corresponding C 1*s* peak. No finer details in the XA peak are seen. The XP peak position is in this case located rather high up at the leading edge of the absorption peak. This is most pronounced in grazing incidence.

The oxygen edge peak is about as broad as the nitrogen peak. The O 1*s* XPS peak (FWHM $=1.07$ eV), however, is even broader than the N 1*s* peak. As in the other cases the leading edge changes somewhat depending on the polarization. The XPS position falls almost at the top of the edge at grazing incidence and at normal incidence the XPS and XAS peak positions more or less exactly coincide.

We interpret the peak at the Fermi level as due to adsorbate unoccupied 2*p*-metal 3*d* hybrid states, see Sec. III A. As discussed in Sec. III B this part of the spectrum may be significantly perturbed relative to the unoccupied adsorbate-*p* projected density of states due to dynamic effects. In the static final-state picture the distribution of final states can to a good approximation be obtained by applying the $Z+1$ approximation. This implies in the present case that the C 1*s*, N 1*s*, and O 1*s* final states behave very much like adsorbed nitrogen, oxygen, and fluorine atoms, respectively. The XA spectral shapes should thus be similar to the distribution of empty states, as, e.g., measured by inverse photoemission, for the next element in the series. This means, for instance, that the XA spectrum for adsorbed carbon should be compared to the inverse photoemission spectrum for nitrogen, and the

XA spectrum for nitrogen should be compared to the inverse photoemission spectrum for oxygen, etc.

As we go from carbon to nitrogen to oxygen the leading edges get successively broader. This is the same trend as seen in XPS. The broadenings of the spectra are consistent with the assumption that the XAS broadening at threshold is almost identical to the XPS broadening.[2,7] The XPS linewidths are dominated by vibrational effects.[17] The similar behavior of the XPS broadenings and the broadening of the XA leading edges thus suggests that the edges are influenced by the same type of vibrational effects. In order to test this assumption, the XA spectra were recorded at different temperatures.

In Fig. 7 the C 1*s*, N 1*s*, and O 1*s* XA edge features recorded at low and high temperature are compared. The spectra are not calibrated to each other to high accuracy, so the relative positions of the spectra at the different temperatures may be incorrectly reproduced. In the nitrogen and oxygen spectra pronounced and reversible temperature effects are seen. For carbon the width of the leading edge does not change significantly, whereas the FWHM of the absorption feature increases slightly. When compared to the previously measured temperature effects in XPS core-level spectra, we find that the temperature-dependent broadenings are consistent in the two sets of spectra. This overall similarity clearly indicates that the edges are vibrationally broadened in the same way as the XP final states.[17]

For the presently investigated atomic adsorbates we

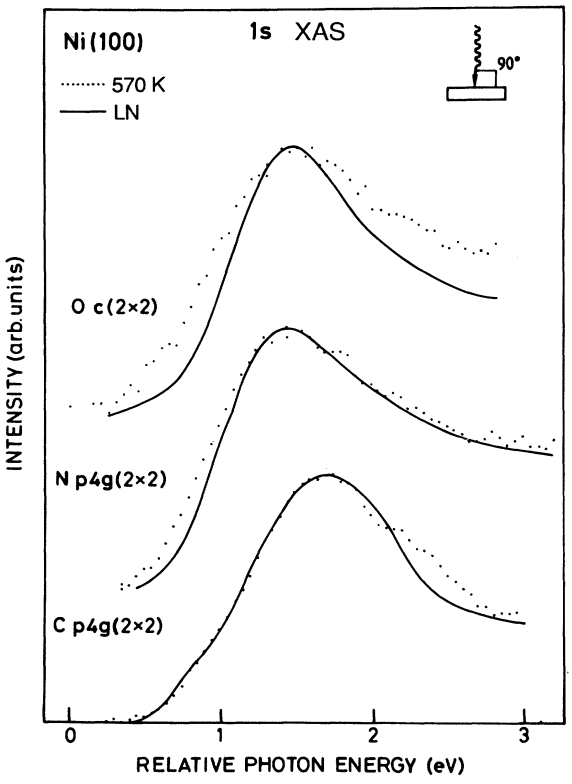

FIG. 7. XA spectra of C, N, and O on Ni(100) heated to 570 K and cooled by liquid nitrogen.

may expect the vibrational effects to be rather similar over the edge peaks. The 1*s* core electron is excited to a mainly antibonding (possibly nonbonding) 2*p*-derived final state. The main difference for the excitations which are situated further away from threshold but still within the first resonance, is that the states may be somewhat different in terms of the character of the 2*p*-3*d* hybridization. From the comparison with the XPS line profiles and from the magnitude of the observed temperature effects, it is clear that C 1*s* XA spectrum is little affected by vibrational effects, whereas the N 1*s* and O 1*s* spectra are significantly influenced.

As referred to above it is important to remember that for metallic systems the lowest core-hole state is the same for XAS and XPS.[2] The exact relation between edge and the XPS binding energy is modified by the broadenings and dynamic effects discussed above (Sec. III B). This will now be discussed with respect to the atomic adsorbates investigated. In an idealized case with a constant density of states in the region close to the Fermi level, no dynamic effects and a symmetric broadening due to the core hole in the XA and XP spectra, the XPS peak (the Fermi level) will be located halfway up on the edge. However, as soon as the density of states (DOS) is not constant this will be modified. Especially if the DOS is narrow compared to the XPS line profile, the Fermi level will correspond to the first peak in the XA spectrum. One reason for sharp features in the XA spectrum may be due to dynamical effects. Based on the XPS binding energies, we locate the Fermi level for the XA spectra at 283.0, 397.3, and 530.1 eV for the C 1*s*, N 1*s*, and O 1*s* levels, respectively. In Figs. 4–6 there are obviously different energy relationships between the XA and XP spectra. Considering the widths of the XPS profiles it is seen that the width of the 2*p*-3*d* hybrid state to which the XA excitation is made is continuously getting narrower as we go from carbon to oxygen.

In the case of carbon the spectrum seems to be well described by an unoccupied density of states to which excitations are made. The XPS binding energy also corresponds to a distinct signature in the XAS edge giving further support for the identity between the XPS and XAS energy scales. The dynamic effects are probably of importance for the shape of the spectrum, and it may be that the kink at the Fermi level is influenced by this. In the carbon adsorbate we expect the 2*p* band to be more than half filled. With the type of discussion in the previous section in connection to Fig. 2, it is seen that if a carbon atom on the surface has approximately a negative charge of one[43] and the core hole is screened by almost one 2*p* electron the part of the intensity which is connected to the dynamic effects is on the order of 30% (corresponding to the shaded region in Fig. 2). As will be discussed below, the spectral feature around 10 eV also contains empty 2*p* states. It is plausible that the dynamic effects influence the edge peak more, which means that the weight in this region may be much enhanced relative to the projected *p* density of states for the final state (which should be similar to the ground-state density of states for nitrogen).

In the nitrogen spectrum it is seen that the XPS peak

position has moved much higher up on the XAS profile. Using the $Z+1$ approximation, nitrogen with a core hole should be compared with oxygen. Inverse photoemission results for O/Ni(100) show adsorbate-induced states in a narrow range at the Fermi level.[22] The widths of the unoccupied $2p$ bands can be expected to decrease from carbon to oxygen because they are getting successively more filled. This also means that the spectral weight related to the dynamical effects are getting more pronounced so that much of the intensity at the nitrogen absorption may be related to these effects. In both polarizations, however, the XA peaks are broader than the XPS peak demonstrating the presence of both $2p_{xy}$-$3d$ and $2p_z$-$3d$ hybrid states.

For oxygen, the XPS peak position almost coincides with the peak position of the XAS edge feature. This is most pronounced in the normal incidence spectrum where they coincide totally. This part of the spectrum looks much like the case which was demonstrated in Fig. 3 for Ni, where we have almost a complete closing of the band when the core hole is created. When we create a core hole on the oxygen the final state becomes fluorine-like and we do indeed expect this final state to have essentially a filled $2p$ band. If we first consider the normal incidence spectrum it could be explained if it is assumed that there are essentially no empty $2p_{xy}$-$3d$ hybrid states leading only to the appearance of a peak at the edge as in Ni. The edge feature is somewhat broader than the XPS peak but a large fraction of the total width is due to this, i.e., to vibrations. The spectrum recorded at grazing incidence is both broader and more intense. The width of the peak implies that there is hybridization between the $2p_z$ and the $3d$ orbitals leading to some empty $2p_z$-derived states in the core-hole state. The intensity enhancement in this polarization is partly due to this empty density of states but it could also indicate that $2p_z$ is more involved in the screening of oxygen core hole than are the $2p_{xy}$ orbitals.

An important conclusion from the results in this section is that the comparison between the spectra and calculated density-of-states curves (from orbital energy calculations or multiple-scattering calculations) may be much influenced by dynamical effects. For these systems in which the $2p$ band is close to being filled the relative influence of these effects may even dominate certain parts of the spectra. A quantitative study of the empty $2p$-derived states with photoabsorption especially may lead to large relative errors if these effects are not taken into account.

B. Higher excited states

In Fig. 8 XA spectra of C, N, and O in the region up to 20 eV or more above the edges are shown on a common energy scale, formed by subtracting the XPS binding energies from the photon-energy scales. The spectra are recorded both for grazing and normal incidence. The spectral features show some similarities between the different adsorbates, and can be divided into three regions. The first region extends from threshold up to approximately 2.5 eV. This part of the spectra has been discussed in the preceding section. A second region can be discerned between 2.5 and 6 eV above the edge. The observed structures decrease in intensity relative to the other parts of the spectra when going from C to O. A third region extends towards higher energies, and contains broad features between 6 to 12 eV. These features are mainly observed for light incident normal to the surface. Furthermore, very broad features are seen at higher energies.

Before proposing assignments to the states in regions 2 and 3, we will discuss some of the higher excited states seen in free molecules containing C, N, and O. In CO and N_2 there exist three types of higher excited states above threshold (which in this case corresponds to the lowest unoccupied orbital, $2\pi^*$).[44] At high energies, well above the ionization limit, a $2p$-derived state of σ symmetry is observed. Since this state resides in the ionization continuum, it has been denoted a shape resonance and can be described as an antibonding orbital between the two atoms. It is plausible that similar resonances can be

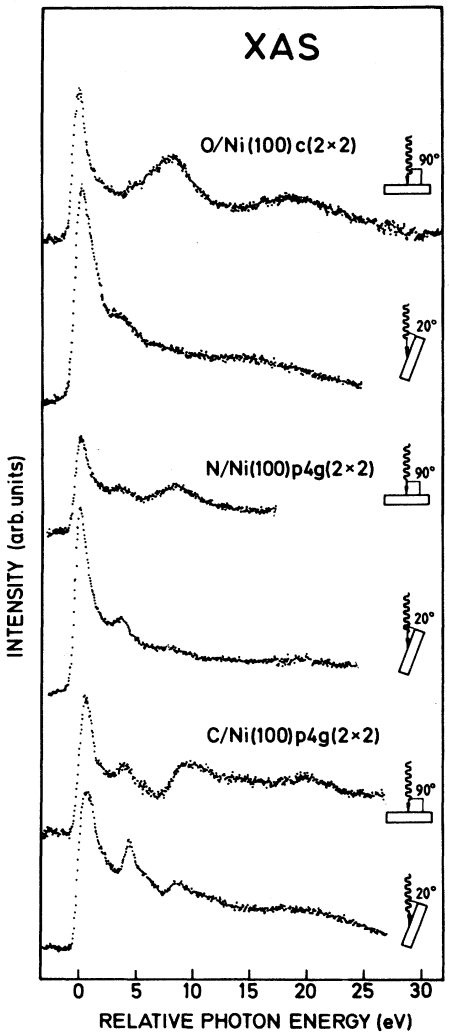

FIG. 8. XA spectra for C, N, and O adsorbed on Ni(100). The zero of the energy scale corresponds to the respective XPS binding energies.

found in the atomic adsorbates related to the empty 2*p*-Ni *sp* antibonding states depicted in Fig. 1 high above the Fermi level.

In the free molecular spectra sequences of excitations to Rydberg states are observed, which converge towards the ionization limits. These molecular orbitals are derived from 3*p* to *np* atomic orbitals. The intensity in the absorption spectra related to these orbitals are to a first approximation expected to remain constant independent of chemical surrounding (see Sec. III B). In the adsorbate case, the excitations to 3*p* and higher *np* states must give rise to intensity in the spectrum. Even though the states may be shifted and broadened due to hybridization with the substrate orbitals, thereby no longer being pure Rydberg orbitals, the states are not quenched.[8]

The free molecular spectra also contain multielectron states which do not correspond to simple orbital excitations. These are attributed to valence excitations accompanying the main core excitation. Such processes where low-energy excitations across the Fermi level take place are the cause of the dynamical effects in the XA spectra (Sec. III B) and is one source of asymmetry in XPS. In addition to such low-energy excitations high-energy multielectron excitations, shake-up satellites, have been observed in the core ionization (XP) spectra of the atomic adsorbates.[23] It is expected that similar processes also occur in the core excitation (XA) spectra although their intensities may be totally different.

We propose that the spectral structures seen in region 2 (2.5–6 eV) can be attributed to excitations to higher *p* states, i.e., 3*p*, 4*p*, etc. The large size of these higher atomic orbitals makes them hybridize with Ni states, in particular with the spatially more extended Ni 4*sp* states. These *np* derived states therefore form a broad band. Only the states below the ionization limit (vacuum level) will be bound states, whereas the higher states are transformed into continuum resonances. These resonances will have a short lifetime due to the decay of the excited electron into the free-electron continuum, in analogy with the above discussed strongly lifetime broadened shape resonances. In the case of molecular-orbital shape resonances, however, the lifetime is somewhat increased due to the presence of a centrifugal barrier, allowing the state to be observed. For the *np* states above the ionization limit the lifetime will be shorter, resulting in very broad, unobservable spectral features. The work function of the clean Ni(100) surfaces is 5.5 eV (Ref. 45) (Godby[46] uses 5.1 eV) and the work-function change upon adsorption of O is about +0.35 eV.[46,47] For carbon the increase is smaller, 0.1 eV,[45] and for nitrogen we are not aware of any data. We estimate that the ionization limit is somewhere between 5 and 6 eV above the Fermi level. The spectral features in region 2 should then correspond to the bound part of the *np* derived states.

As pointed out earlier, the *np* derived states in region 2 become more difficult to observe from C to O. If the atomic cross section for *np* states were constant for C, N, and O the reverse would be observed, since the 2*p* intensity should diminish when the 2*p*-derived states become more occupied when going from C to O. The observed effect can be related to the fact that the 1*s* orbital is considerably smaller in O than in C, causing a reduced intensity of the *np* states due to smaller core to valence wavefunction overlap as discussed in Sec. III B. There is also a variation in the *np*-derived intensity with the angle of the incoming light. The states are sharper and more intense for grazing incidence where we excite to *np* states perpendicular to the surface. This effect is most clearly seen in the case of C. This indicates that the perpendicular np_z is less hybridized with the substrate. The existence of higher 3*p* and *np* states were predicted in a previous core ionization shake-up study of the C, N, and O on Ni(100).[23] The major satellites were assigned to 2*p*-*np* excitations.

Region 3 can be related to the antibonding 2*p*-Ni 4*sp* hybrid states which are located above the ionization limit (see Sec. III A). The $2p_{x,y}$ orbitals are probed in normal incidence and the $2p_z$ orbital in grazing incidence with the polarization vector perpendicular to the surface. Following the description from free molecules, these states can be denoted shape resonances. The shape resonance is an antibonding state, and the intensity can thus be related to the degree of participation of a specific 2*p* atomic orbital in the bonding of the surface.

The shape resonances are relatively strong in normal incidence, and can be observed as broad structures centered at 8.3 eV for both O and N and at 9.6 eV for C in Fig. 8. In grazing incidence there is no structure seen in the oxygen spectrum, and only a very weak feature in the N spectrum at 8.3 eV. The carbon spectrum, on the other hand, shows a stronger feature located at 8.6 eV which is a shift of 1 eV towards lower energy compared to normal incidence.

The observation of an enhancement of the shape resonance in normal incidence can be anticipated considering the local adsorption site. Overlap of the adsorbate 2*p* orbitals with surrounding nickel atoms is necessary for the formation of a centrifugal barrier in this case as well as for bonding (and antibonding) interaction. The presence of an enhancement of the absorption in normal incidence therefore shows that mainly the $2p_{x,y}$ orbitals are involved in the bonding to the substrate. In the case of O, no shape resonance can be observed in grazing incidence indicating a smaller participation of the $2p_z$ component in this type of O 2*p*-Ni 4*sp* bonding. Cluster calculations of the atomic adsorbates on a Ni(100) surface have shown that the O $2p_z$ orbital can be considered as a filled lone pair orbital.[43] The involvement of the $2p_z$ orbital in the bonding becomes slightly apparent in N and increases further in C. In the latter case the energy shift of the shape resonance in grazing incidence indicates the existence of a different antibonding state. The reconstruction of the Ni surface lattice upon adsorption of C and N allows the adsorbate to be accommodated within the first Ni layer. The $2p_z$ orbital can then have a substantial overlap with a fifth Ni atom, situated below the adsorbate in the second Ni layer. Cluster calculations of N and C adsorption show that it is the participation of the $2p_z$ orbital in bonding to the fifth atom which increases the adsorption energy, and is the driving force for the reconstruction.[43] These observations are consistent with the

observation of sharper *np* states for grazing than for normal incidence (cf. above). However, for oxygen the peak just above the threshold was found to be stronger and broader at grazing incidence. According to the selection rules this should be related to the O $2p_z$ orbital and imply a larger hybridization than for O $2p_{xy}$. It is plausible that the O $2p_z$ lone pair orbital is mainly responsible for the $2p$-Ni $3d$ hybridization, forming a band centered around the Fermi level, as discussed in Sec. IV A. The apparent weight of the $2p$-Ni $3d$ hybridization may be enhanced by the narrow width of this band.

The shape resonance state in O has previously been observed in a low-resolution XAS (NEXAFS) study and interpreted using multiple-scattering calculations.[6,48] However, the state was not denoted a shape resonance, but was instead attributed to multiple-scattering processes. The two pictures may be made compatible; the multiple-scattering calculation can be regarded as an approach to obtain the band structure of the empty states, and in the shape resonance picture, the O $2p$ states do not only hybridize with the nearest Ni neighbors in the hollow site, but with the whole *sp* band which extends over several substrate atoms. There are states, however, which can be difficult to account for in a multiple-scattering calculation, such as the extended states made up of *np* atomic orbitals and Ni $4sp$ states.

V. CONCLUSIONS

We have demonstrated the importance of considering dynamical threshold effects in XA spectra of chemisorbates. Instead of the XA spectra simply reflecting the unoccupied density of states, these effects redistribute some of the intensity to form a spectral singularity at threshold. The effects will be most important when there is a low density of states just above the Fermi level, as in, for instance, O/Ni(100) and Ni metal. Furthermore, the threshold will be broadened by vibrational excitations, related to similar phenomena in core ionization. The vibrational broadening is seen to increase when going from C to O.

Higher *np*-derived states are observed above the threshold region. They are best seen at grazing incidence and decrease in intensity when going from C to O. These states are only observed as bound states below the adsorbate ionization limit. At higher energies, the presence of $2p$-derived shape resonances is proposed. These consist mainly of the $2p_{xy}$ component parallel to the surface plane. In the case of C/Ni(100), a contribution from the $2p_z$ component can also be discerned. This can be related to bonding to second-layer Ni atoms. The p_{xy} shape resonance corresponds to x-y scattering paths in the multiple-scattering picture of NEXAFS. The relative contribution from $2p_{xy}$ and $2p_z$ orbitals of the bonding is discussed.

ACKNOWLEDGMENTS

This work was supported by the Swedish Natural Science Research Council (NFR) and th Swedish National Board for Industrial and Technical Development (NUTEK). We are indebted to the staff at MAX-lab for the excellent facilities put to our disposal.

[1]J. Stöhr, *NEXAFS Spectroscopy*, Springer Series in Surface Science Vol. 25 (Springer-Verlag, Heidelberg, 1992).
[2]A. Nilsson, O. Björneholm, E. O. F. Zdansky, H. Tillborg, N. Mårtensson, J. N. Andersen, and R. Nyholm, Chem. Phys. Lett. **197**, 12 (1992).
[3]N. Wassdahl, A. Nilsson, T. Wiell, H. Tillborg, L.-C. Duda, J. H. Guo, N. Mårtenson, J. Nordgren, J. N. Andersen, and R. Nyholm, Phys. Rev. Lett. **69**, 812 (1992).
[4]O. Björneholm, A. Sandell, A. Nilsson, N. Mårtensson, and J. N. Andersen, Phys. Scr. **T41**, 217 (1992).
[5]N. Mårtensson and A. Nilsson, J. Elecron. Spectrosc. Relat. Phenom. **52**, 1 (1990).
[6]D. Norman, J. Stöhr, R. Jaeger, P. J. Durham, and J. B. Pendry, Phys. Rev. Lett. **51**, 2052 (1983).
[7]O. Björneholm, A. Nilsson, E. O. F. Zdansky, A. Sandell, B. Hernnäs, H. Tillborg, J. N. Andersen, and N. Mårtensson, Phys. Rev. B **46**, 10 353 (1992).
[8]O. Björneholm, A. Nilsson, E. O. F. Zdansky, A. Sandell, H. Tillborg, J. N. Andersen, and N. Mårtensson, Phys. Rev. B **47**, 2308 (1993).
[9]M. Bader, C. Ocal, B. Hiller, J. Haase, and A. M. Bradshaw, Phys. Rev. B **35**, 5900 (1987).
[10]H. Onuferko, D. P. Woodruff, and B. W. Holland, Surf. Sci. **87**, 357 (1978).
[11]L. Wenzel, D. Arvanitis, W. Daum, H. H. Rotermund, J. Stöhr, K. Baberschke, and H. Ibach, Phys. Rev. B **36**, 7689 (1987).
[12]J. E. Demuth, D. W. Jepsen, and P. M. Marcus, Phys. Rev. Lett. **31**, 540 (1973).
[13]M. Rocca, S. Lehwald, H. Ibach, and T. S. Rahman, Phys. Rev. B **35**, 9510 (1987).
[14]M. Rocca, S. Lehwald, and H. Ibach, Surf. Sci. Lett. **163**, L738 (1985).
[15]W. Daum, S. Lehwald, and H. Ibach, Surf. Sci. **178**, 528 (1986).
[16]A. L. D. Kilcoyne, D. P. Woodruff, A. W. Robinson, T. Lindner, J. S. Somers, and A. M. Bradshaw, Surf. Sci. **253**, 107 (1991).
[17]A. Nilsson and N. Mårtensson, Phys. Rev. Lett. **63**, 1483 (1989).
[18]Y. Gauthier, Surf. Sci. **251/252**, 493 (1991).
[19]W. Oed, H. Lindner, U. Starke, K. Heinz, K. Müller, and J. B. Pendry, Surf. Sci. **224**, 179 (1989).
[20]J. Stöhr, R. Jaeger, and T. Kendelewicz, Phys. Rev. Lett. **49**, 142 (1982).
[21]A. L. D. Kilcoyne, D. P. Woodruff, J. E. Rowe, and R. H. Gaylord, Phys. Rev. B **39**, 12 604 (1989).
[22]H. Scheidt, M. Glöbl, and V. Dose, Surf. Sci. Lett. **123**, L728 (1982).
[23]A. Nilsson and N. Mårtensson, Chem. Phys. Lett. **182**, 147 (1991).
[24]R. Nyholm, S. Svensson, J. Nordgren, and S. A. Flodström, Nucl. Intrum. Methods **A246**, 267 (1986).
[25]J. N. Andersen, O. Björneholm, A. Sandell, R. Nyholm, J.

Forsell, L. Thånell, A. Nilsson, and N. Mårtensson, Synchrotron Radiat. Res. **4**, 15 (1991).
[26]R. N. S. Sodhi and C. E. Brion, J. Electron Spectrosc. Relat. Phenom. **34**, 363 (1984).
[27]R. W. Godby, G. A. Benesh, R. Haydock, and V. Heine, Phys. Rev. B **32**, 655 (1985).
[28]C. S. Wang and A. J. Freeman, Phys. Rev. B **19**, 4930 (1979).
[29]D. E. Eastman and J. K. Cashion, Phys. Rev. Lett. **27**, 1520 (1971).
[30]F. M. F. de Groot, M. Grioni, J. C. Fuggle, J. Ghijsen, G. A. Sawatsky, and H. Petersen, Phys. Rev. B **40**, 5715 (1989).
[31]D. W. Bullet and W. G. Dawson, Vacuum **38**, 385 (1988).
[32]C. F. McConville, D. P. Woodruff, S. D. Kevan, M. Weinert, and J. W. Davenport, Phys. Rev. B **34**, 2199 (1986).
[33]J. Somers, A. W. Robinson, T. Lindner, D. Ricken, and A. M. Bradshaw, Phys. Rev. B **40**, 2053 (1989).
[34]H. Ågren, J. Nordgren, L. Selander, C. Nordling, and K. Siegbahn, Phys. Scr. **18**, 499 (1978).
[35]J. Stöhr and R. Jaeger, Phys. Rev. B **26**, 4111 (1982).
[36]U. von Barth and G. Grossman, Solid State Commun. **32**, 645 (1979).
[37]U. von Barth and G. Grossman, Phys. Rev. B **25**, 5150 (1982).
[38]G. D. Mahan, Phys. Rev. **163**, 612 (1967).
[39]P. W. Anderson, Phys. Rev. Lett. **18**, 1049 (1967).
[40]P. Nozières and C. T. DeDominicis, Phys. Rev. **178**, 1097 (1969).
[41]B. Hernnäs, O. Björneholm, A. Nilsson, H. Tillborg, A. Sandell, M. Karolewski, N. Mårtensson, and J. N. Andersen, Phys. Rev. B **47**, 16 052 (1993).
[42]For the carbon covered surface we found a significant intensity increase on the high-energy side of the Ni $2p_{3/2}$ absorption edge peak. This was observed in total yield spectra recorded with lower resolution to monitor changes in the photon energy. The effect has not been investigated further for this system.
[43]I. Panas, J. Schüle, U. Brandemark, P. Siegbahn, and U. Wahlgren, J. Phys. Chem. **92**, 3079 (1988).
[44]A. P. Hitchcock and C. E. Brion, J. Electron Spectrosc. Relat. Phenom. **18**, 1 (1980).
[45]K. C. Prince, M. Surman, T. Lindner, and A. M. Bradshaw, Solid State Commun. **59**, 71 (1986).
[46]R. W. Godby, Phys. Rev. B **32**, 5432 (1985).
[47]T. D. Pope, S. J. Bushby, K. Griffiths, and P. R. Norton, Surf. Sci. **258**, 101 (1991).
[48]D. D. Vvedensky and J. B. Pendry, Surf. Sci. **162**, 903 (1985).
[49]A. Bosch, H. Feil, G. A. Sawatsky, and N. Mårtensson, Solid State Commun. **41**, 355 (1982).